Arabian Journal of Chemistry (2019) **12**, 4957–4970

King Saud University

Arabian Journal of Chemistry

www.ksu.edu.sa
www.sciencedirect.com

ORIGINAL ARTICLE

N,N-dimethylformamide (DMF), and N,N-dimethylacetamide (DMA) reactions with NO_3, OH and Cl: A theoretical study of the kinetics and mechanisms

S. Samai [a], **S. Rouichi** [a], **A. Ferhati** [a,*], **A. Chakir** [b]

[a] *LCCE Laboratoire de chimie et chimie de l'environnement, faculté des sciences, département de chimie, université de Batna, 05000 Batna, Algeria*
[b] *GSMA, UMR CNRS 6089, UFR Sciences, université de Reims, BP 1039, 51687 Reims Cedex 2, France*

Received 23 August 2016; accepted 21 October 2016
Available online 9 November 2016

KEYWORDS

Amide;
CBS-QB3;
Kinetics;
Mechanism;
OH radical;
Nitrate radical;
Chlorine atom;
Rate constant

Abstract A theoretical study of the kinetics and the mechanism of the hydrogen abstraction by OH, Cl and NO_3 radicals from two amides (DMF and DMA) has been investigated. Calculations were carried out using DFT B3LYP/6-311 + + G(2d,pd)/CBS-QB3 and transition-state theory. This work provides the first theoretical determination of the rate coefficients and detailed mechanism for the reactions of OH, NO_3 radicals and chlorine atoms with DMF/DMA, over a temperature range 273–380 K and at atmospheric pressure. The obtained rate coefficients are in reasonable agreement with experiments. Results indicate that the mechanism of the Cl and NO_3 reactions with amides goes preferentially through H-abstraction from (C(O)H) and ($C(O)CH_3$) groups. Meanwhile the mechanism of the OH with amides (DMF, DMA) is dominated by H-abstraction from the N-methyl groups.

1. Introduction

Amides constitute a large variety of Nitrogen Volatil Organic Compounds (NVCOs) that are considered as tropospheric contaminants. These compounds are emitted into the atmosphere as primary pollutants from several sources including the petrochemical industry, the microelectronics fabrication industry, as well as the manufacture of various products such as synthetic polymers, dyes, cosmetics, drugs, and pesticides (Manahan, 1994; Finlayson-Pitts and Pitts, 1999; Carter, 1994). They are also formed in situ as intermediate products upon the atmospheric degradation of several important amines or pesticides (Finlayson-Pitts and Pitts, 1999; Tuazon et al., 1994). In the troposphere the potential removal processes of these compounds

* Corresponding author.
E-mail address: azeddine.ferhati@univ-batna.dz (A. Ferhati).
Peer review under responsibility of King Saud University.

Production and hosting by Elsevier

http://dx.doi.org/10.1016/j.arabjc.2016.10.012
1878-5352

are mainly chemical reactions with OH, Cl and NO_3 radicals. The determination of the kinetic rate constants and mechanisms of degradation is of great importance since it constitutes the only route through which we may assess the fate of these contaminants once they are emitted to the troposphere. This fate is expressed in terms of their persistence and tropospheric lifetimes with respect to each atmospheric photo-oxidant. Unfortunately, studies concerning the kinetics of degradation of amides are scarce.

The reaction of amides with atmospheric oxidants has been studied by Koch et al. (1997), Aschmann and Atkinson (1999), Solignac et al. (2005), and El Dib and Chakir (2007). Koch et al. (1997) investigated the kinetics of oxidation of several amides by OH-radicals at different temperatures using flash photolysis/resonance fluorescence. Aschmann and Atkinson (1999) investigated the kinetics of homogeneous OH and NO_3 oxidation of 1-methyl-2 pyrrolidinone, a cyclic amide, using the technique of relative rates. Solignac et al. (2005) investigated the kinetics of oxidation of amides at room temperature by OH radicals and also by chlorine atoms. The experimental approach used being the technique of a simulation chamber coupled to an FTIR spectrometer. Meanwhile, El Dib and Chakir (2007) reported the rate coefficient for the reaction of NO_3 radicals with several amides at different temperatures using laser photolysis coupled with time resolved absorption UV–visible spectroscopy. The kinetic results of these studies show that the degradation of amides by atmospheric oxidants is sensitive to the amide structure. In addition, these reactions proceed via H-atom abstraction at any and all sites containing an H-atom. In their mechanistic studies of the reactions of amides with OH Solignac et al. (2005) observed that the major channel appears to be abstraction from methyl groups attached to the nitrogen atom. However, it should be noted that H-abstraction from other groups may occur particularly in the case of DMF due to the liability of the H-atom in the C(O)H group. At present, we cannot confirm or refute any of the proposed OH-degradation mechanisms of amides. Further mechanistic and theoretical investigations are required to provide a much improved understanding of the mechanism of amide reactions with OH, NO_3 radicals and Cl atoms. To the best of our knowledge, there are no theoretical studies concerning the reaction of amides with OH, Cl and NO_3 radicals up to now. The present work reports the first theoretical study regarding the kinetics of the reactions of OH, NO_3 radicals and Cl atoms with DMF $(CH_3)_2NC(O)H$ and DMA $(CH_3)_2NC(O)CH_3$). The purpose of this work was to provide kinetic data for reactions **I** and **II** and to estimate the branching ratios for the different paths contributing to the overall reactions.

$$(CH_3)_2NCOH + X(OH,NO_3,Cl) \rightarrow (CH_3)(\cdot CH_2)NCOH + HX \quad (\boldsymbol{I_{x-DMF}})$$
$$\rightarrow CH_3)_2NC{\cdot}O + HX \quad (\boldsymbol{II_{x-DMF}})$$
$$(CH_3)_2NC(O)CH_3 + X(OH,NO_3,Cl) \rightarrow (CH_3)(\cdot CH_2)NC(O)CH_3 + HX \quad (\boldsymbol{I_{x-DMA}})$$
$$\rightarrow (CH_3)_2NC(O)\cdot CH_2 + HX \quad (\boldsymbol{II_{x-DMA}})$$

2. Theoretical methods

2.1. Quantum chemistry calculations

Calculations were carried out using Gaussian 09 package (Gaussian 09, 2010) available in the CLOVIS platform at the University of Champagne-Ardenne in France. The Optimized geometries and electronic structure for all minima and transitions states have been performed with DFT B3LYP/6-311++G(2d,pd) level of theory, i.e., using Becke's three-parameter nonlocal-exchange functional with the nonlocal correlation functional of Lee et al. with the 6-311++G(2d,pd) basis set Lee et al. (1988).

The nature of each stationary point was defined by calculating harmonic vibrational frequencies. Every minimum has real frequencies, and the reaction transition states (TSs) are located using the synchronous transit-guided quasi-Newton technique for the saddle point search (QST3 module in GAUSSIAN-09). Hessian matrix of TS is controlled for the presence of a single negative frequency. Animation of the imaginary frequency, often combined with intrinsic reaction coordinate (IRC) calculations, Gonzalez and Schlegel, 1989, 1990 enabled us to correlate a certain transition structure explicitly with its reactants and products.

The B3LYP method overestimates Hydrogen abstraction reaction energies (Montgomery et al., 1999; Coote et al., 2002; Gutbrod et al., 1996; Olzmann et al., 1997; Fenske et al., 2000a,b; Kroll et al., 2001; Zhang et al., 2002; Kuwata et al., 2003; Cremer et al., 1998; Malick et al., 1998) and hence gives unreliable thermochemical predictions. Therefore, in this work, B3LYP method was used only to optimize neutrals, radicals and transition states geometries, whereas the CBS-QB3 model of Petersson and co-workers (Malick et al., 1998) was used to compute the energies of the different systems studied here. In fact recent studies indicate that the CBS-QB3 method often provides good agreement with experimental reaction energies and barriers for molecules having similar size as those studied in this work (Stipa, 2001; Tiu and Tao, 2006; Robinson and Holbrook, 1972). It should be noted that the energies of all structures were obtained using the CBS-QB3 method and corrected for differences in zero-point vibrational energies scaled by 0.99 (Montgomery et al., 1999). Moreover, the study by Dybala-Defratyka et al. (2004) suggests that errors in CBS-QB3 atomization energies are less than 4 kcal/mol.

Radom and co-workers (Wood et al., 2003) have revealed that for the standard CBS-QB3 method, a correction for spin-contamination in open-shell species must be added to the total energy. Heat of formation for all gaseous species involved in the reaction was calculated based on the procedure described in the literature (Stipa, 2001; Curtiss et al., 1997).

Theoretical enthalpies of formation at 0 K are calculated by subtracting the calculated nonrelativistic atomization energies $\sum D_0$ from known enthalpies of formation of the isolated atoms. For any molecule, such as $A_xB_yH_z$, the enthalpy of formation at 0 K is given by

$$\Delta H_f^0(A_xB_yH_z,0\mathrm{K}) = x\Delta H_f^0(A,0\mathrm{K}) + y\Delta H_f^0(B,0\mathrm{K}) + z\Delta H_f^0(H,0\mathrm{K}) - \sum D_0$$

Theoretical enthalpies of formation at 298 K are calculated as

$\Delta\ H^0{}_f\,(0\ \mathrm{K})$ as follows:

$$\Delta H_f^0(A_xB_yH_z,298\,\mathrm{K}) = \Delta H_f^0(A_xB_yH_z,0\,\mathrm{K}) + \left[H^0(AxByHz,298\,\mathrm{K}) - H^0(AxByHz,0\,\mathrm{K})\right] - x\left[H^0(A,298\,\mathrm{K}) - H^0(A,0\,\mathrm{K})\right] - y\left[H^0(B,298\,\mathrm{K}) - H^0(B,0\,\mathrm{K})\right] - z\left[H^0(H,298\,\mathrm{K}) - H^0(H,0\,\mathrm{K})\right]$$

2.2. Rate theory calculations

The rate constant reaction was obtained using RRKM theory (Mokrushin et al., 2002; Tsang et al., 1996; Knyazev and

Tsang, 2000, 1999) with the required sums and densities of states and harmonic frequencies, zero-point energies, moments of inertia, and symmetries essential to determine the kinetic behavior of the reaction were obtained from optimized reactants, transition states, and products calculated with B3LYP/6-311 + + G (2d, pd). Theoretical enthalpies obtained from the CBS-QB3//B B3LYP/6-311 + + G (2d, pd) for all gaseous species involved in the reaction were introduced in the CHEMRATE database.

The calculations were done to determine the temperature dependence of each reaction involved in the mechanism. Further details about of the time-dependent Master Equation (ME) analysis in CHEMRATE are accessible in the literatures (Mokrushin et al., 2002; Tsang et al., 1996; Knyazev and Tsang, 2000, 1999). The precision of the method implemented in CHEMRATE was found to be sufficient through wide comparison with experimental and theoretical data (Tokmakov and Lin, 2003; Tokmakov and Lin, 2004; da Silva, 2009). We did not take into account the low frequency internal rotations as hindered rotors; our simulations take only the most stable conformer. These simplifications will have small influence on numerical accuracy but should not deviate from the validity of rates values.

3. Structural calculations

The calculation involves an examination of the competition between two H- abstraction pathways. For DMF and DMA, there are several sites at which H-abstraction may take place (see Fig. 1). In the case of DMF **(1)**, the reaction is expected to proceed via H-abstraction from either the (-C(O)H) or the (-N(CH_3)$_2$) entities. For DMA **(1′)**, X radicals can abstract the hydrogen atom from (CH_3C(O)-) and (-N(CH_3)$_2$) groups. The transition states (TS) are characterized by a near linear alignment of the radical, the hydrogen to be abstracted, and the central atom of abstraction. The different H-abstraction pathways proceed via two-steps. In the first step, the radical approaches the H atom of the amide, forming an intermediate complex (amide- radical) more energetically stable than the reactants. In the second step of the reaction the intermediate complex dissociates to give reaction products after passing through a transition state (see Figs. 2–9). The H-abstractions were found to be exothermic and exergonic for both species DMF and DMA with all radicals taken in this study.

Table 1 show the energies of reactants and products species involved in the mechanism. The experimental and theoretical enthalpies are in good agreement except for DMFR$_{1–2}$, DMFR$_3$, DMAR$_{1–2}$ and DMAR3 species (Fig. 1) for which the experimental enthalpies are not available in the literatures.

3.1. Reaction with Cl

The energies of all species involved in the H-abstraction reactions are reported in Table 2a, Table 3 and Table 4a, Table 5 for (DMF + Cl) and (DMA + Cl) respectively. The

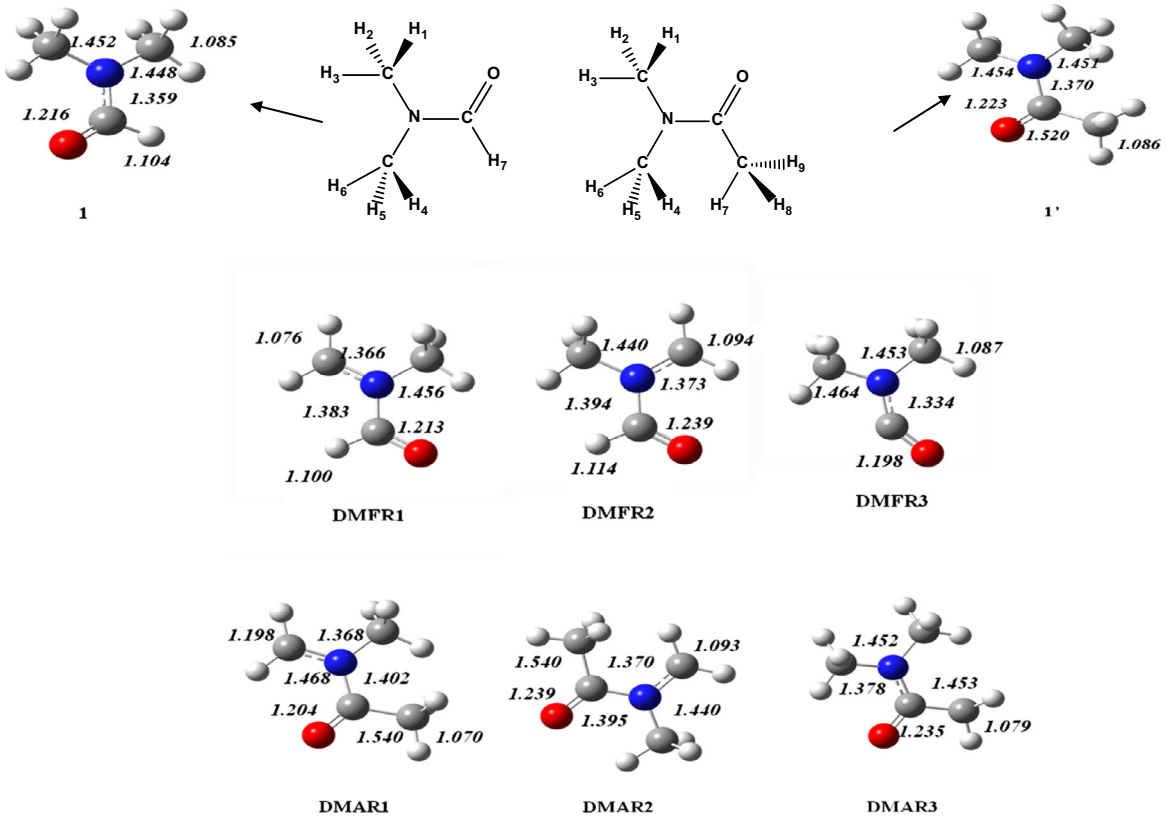

Figure 1 Structures of key species (DMF, DMA) considered for kinetics simulations determined by B3LYP/6-311 + + G(2d,pd), bond lengths in Angstrom.**1**:DMF (CH_3)$_2$NC(O)H), **1′**:DMA((CH_3)$_2$NC(O)CH_3), DMFR1-2:(CH_3)(•CH_2)NC(O)H), DMFR3:((CH_3)$_2$N•C(O), DMAR1-2:(CH_3)(•CH_2)NC(O)CH_3), DMAR3:((CH_3)$_2$NC(O) •CH_2).

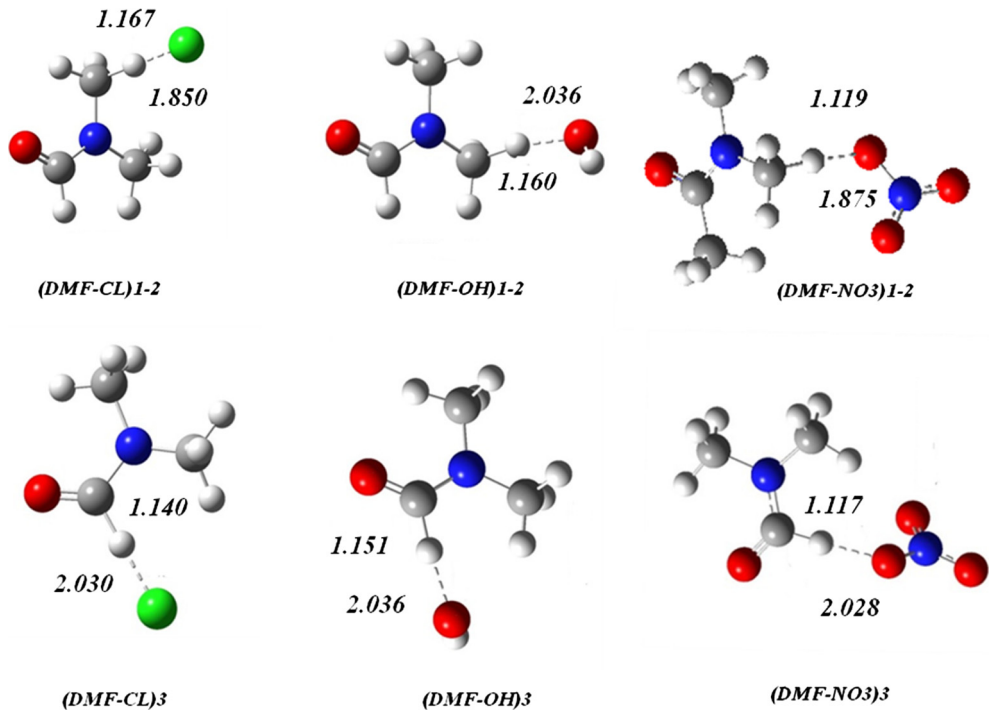

Figure 2 Structures of key species (complex) for reaction DMF + X considered for kinetics simulations determined by B3LYP/6-311 + + G(2d,pd), bond lengths in Angstrom.

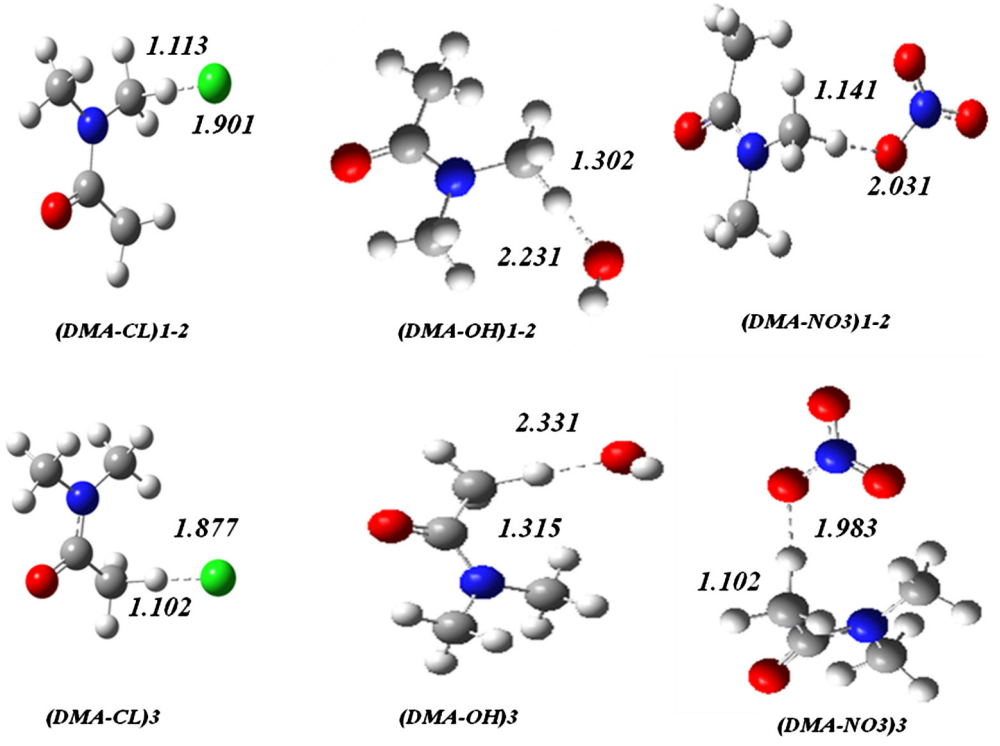

Figure 3 Structures of key species (complex) for reaction DMA + X considered for kinetics simulations determined by B3LYP/6-311 + + G(2d,pd), bond lengths in Angstrom.

mechanism of the reaction of DMF/DMA with Cl is exothermic and occurs via two channels. For the reaction of DMF with Cl, the Cl atom may undergo Hydrogen transfer from DMF (H_{1-6}/H_7), via the H-bonded complexes (DMF- Cl)$_{1-2}$/(DMF- Cl)$_3$ (gain in energy ~10 to 11 kcal mol^{-1}) and $TS_{1-6}Cl$ (abstraction of H_{1-6}) and TS_7Cl (abstraction of H_7) to

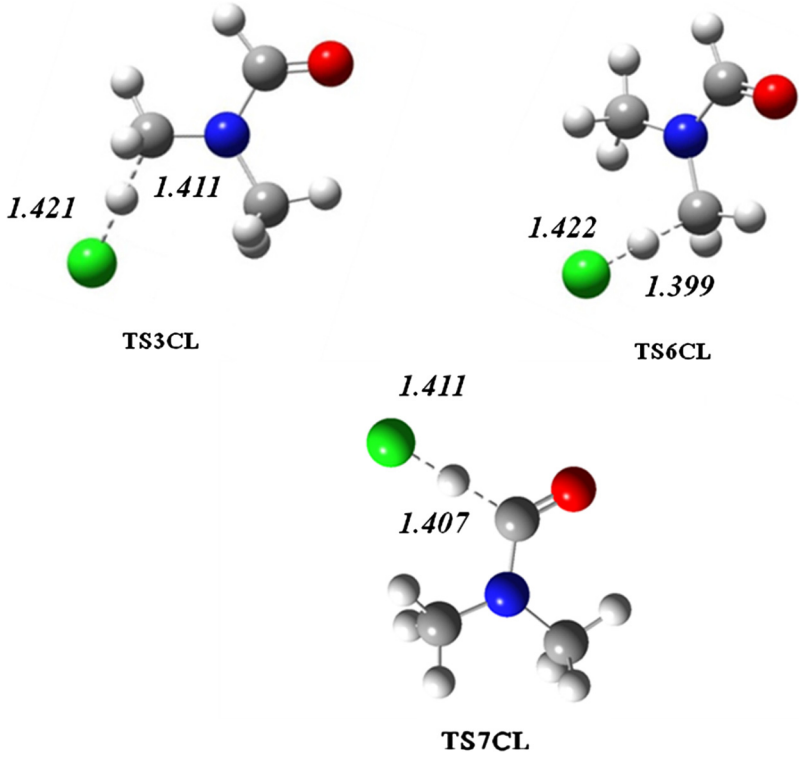

Figure 4 Structures of key species (TS) for reaction DMF + Cl considered for kinetics simulations determined by B3LYP/6-311 + + G (2d,pd), bond lengths in Angstrom.

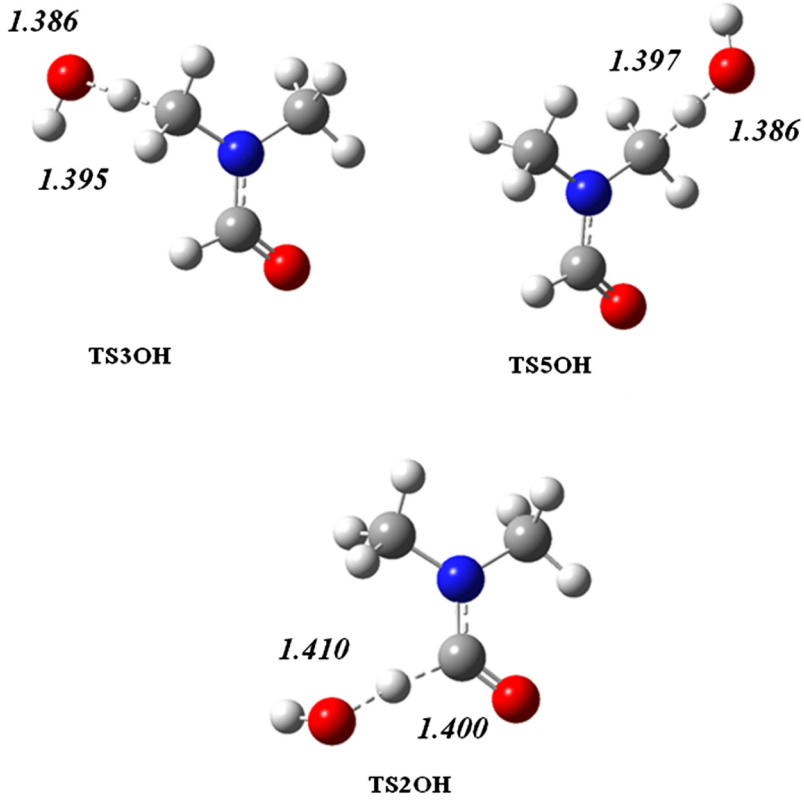

Figure 5 Structures of key species (TS) for reaction DMF + OH considered for kinetics simulations determined by B3LYP/6-311 + + G (2d,pd), bond lengths in Angstrom.

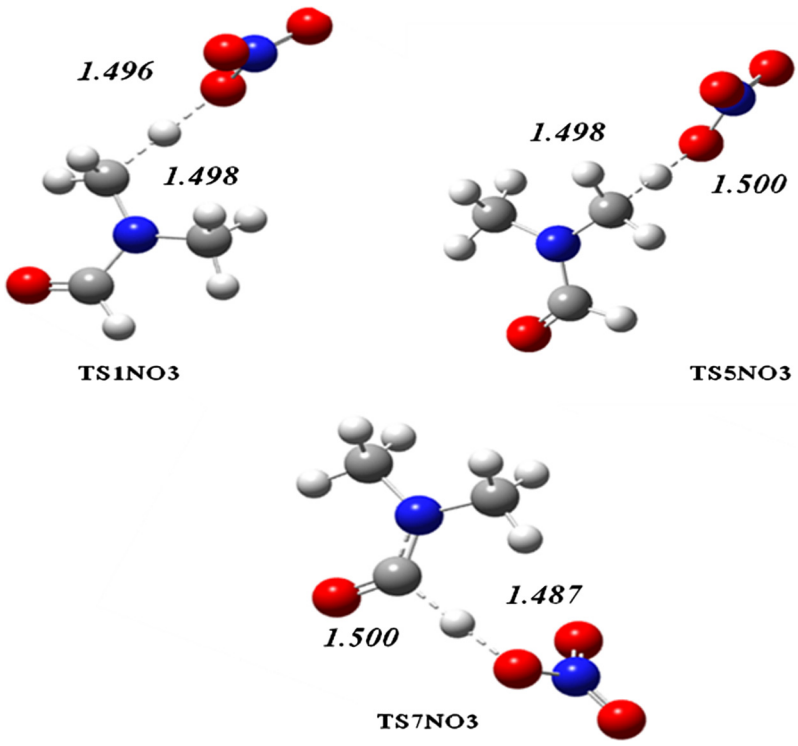

Figure 6 Structures of key species (TS) for reaction DMF + NO_3 considered for kinetics simulations determined by B3LYP/6-311 + + G (2d,pd), bond lengths in Angstrom.

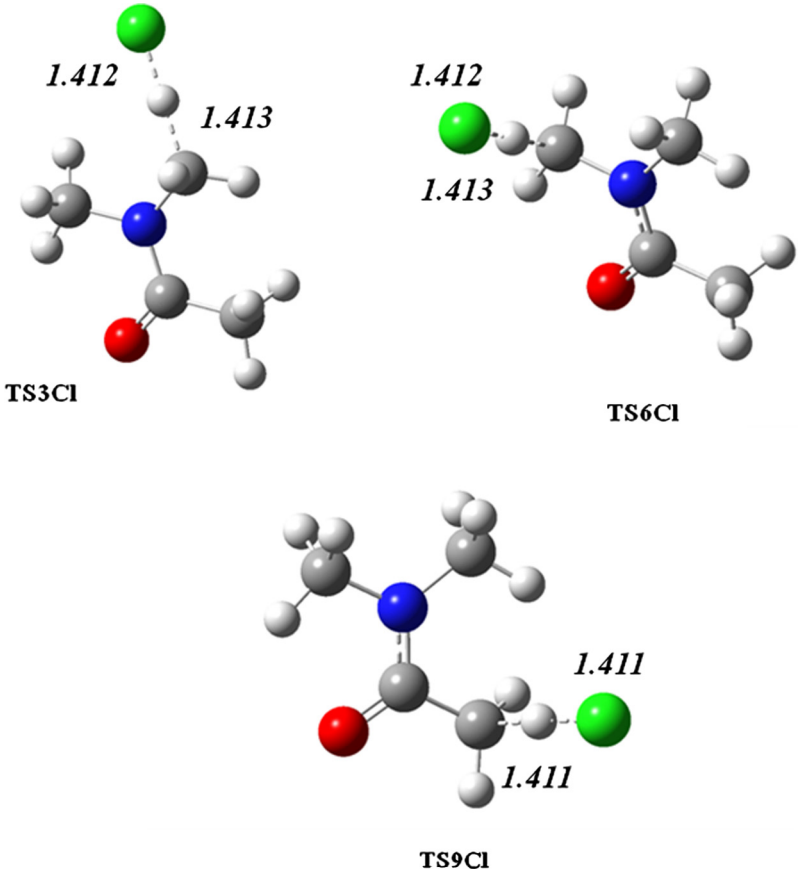

Figure 7 Structures of key species (TS) for reaction DMA + Cl considered for kinetics simulations determined by B3LYP/6-311 + + G (2d,pd), bond lengths in Angstrom.

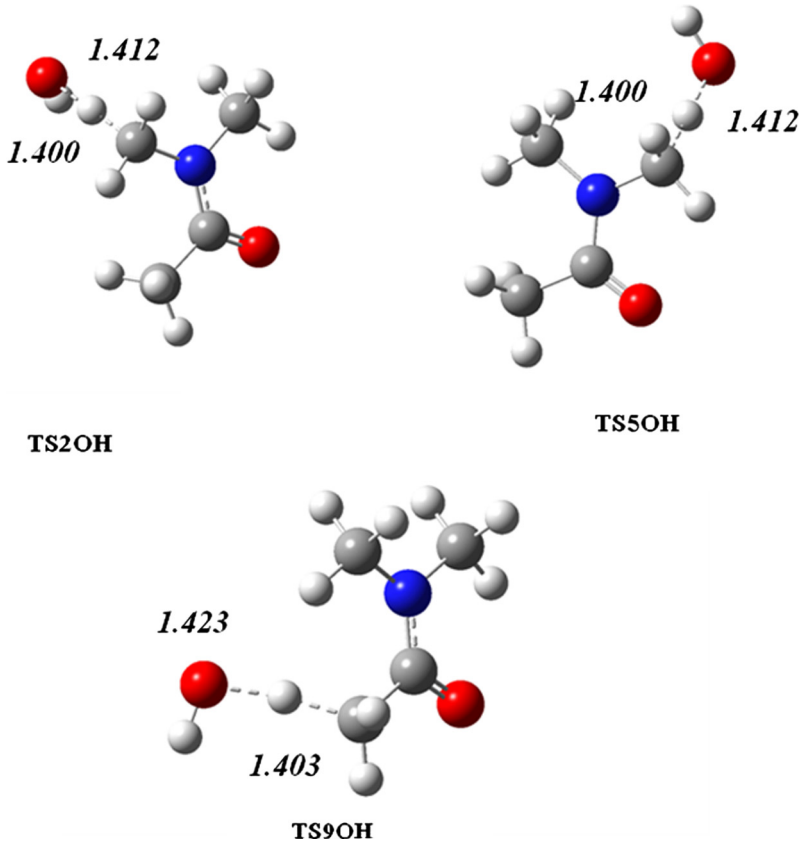

Figure 8 Structures of key species (TS) for reaction DMA + OH considered for kinetics simulations determined by B3LYP/6-311 + + G (2d,pd), bond lengths in Angstrom.

form $DMFR_{1-2}$, $DMFR_3$ and HCl. The energies of $TS_{1-6}Cl$ and TS_7Cl are ~5–8 kcal mol^{-1} higher than the total energy of the reactants.

Hydrogen transfer from DMA(H_{1-6}/H_{7-9}), may also undergo via the H-bonded complexes $(DMA\text{-}Cl)_{1-2}/(DMA\text{-}Cl)_3$ (gain in energy ~5–7 kcal mol^{-1}) and $TS_{1-6}Cl$ (abstraction of H_{1-6}) and $TS_{7-9}Cl$ (abstraction of H_{7-9}) (barrier high ~4 to 10 kcal mol^{-1}) to form $DMAR_{1-2}$, $DMAR_3$ and HCl.

For both DMF and DMA: complexes are characterized by an H—C bond distance of ~1.102 to ~1.167 Å, H—Cl like bond distance of ~1.850 to ~2.030 Å and Cl—H—C bond angle of ~180° respectively; transition states are characterized by an H—C like bond distance ~1.400 to ~1.413 Å, H—Cl like bond distance of ~1.411 to 1.422 Å and Cl—H—C bond angle of ~180° (see Figs. 2–4 and 7).

3.2. Reaction with OH

The energies values are summarized in Table 2b, Table 3 and Table 4b, Table 5 for DMF and DMA, respectively. As for the Cl atom, OH radical also undergoes Hydrogen transfer from DMF (H_{1-6}/H_7), via the H-bonded complexes $(DMF\text{-}OH)_{1-2}/(DMF\text{-}OH)_3$ (gain in energy ~7 to 11 kcal mol^{-1}) and $TS_{1-6}OH$ (abstraction of H_{1-6}) and TS_7OH (abstraction of H_7) to form $DMFR_{1-2}$, $DMFR_3$ and H_2O. The energies of $TS_{1-6}OH$ and TS_7OH are ~4 to 15 kcal mol^{-1} higher than the total energy of the reactants.

Hydrogen transfer from DMA(H_{1-6}/H_{7-9}), similarly in the case of DMF, involves two H-bonded complexes: $(DMA\text{-}OH)_{1-2}/(DMA\text{-}OH)_3$ (gain in energy ~6–8 kcal mol^{-1}) and two transition states: $TS_{1-6}OH$ (abstraction of H_{1-6}) and $TS_{7-9}OH$ (abstraction of H_{7-9}) (barrier high ~14.5–15.5 kcal mol^{-1}) to form $DMAR_{1-2}$, $DMAR_3$ and H_2O.

For both DMF and DMA: complexes are characterized by an H—C bond distance of approximately ~1.150–1.315 Å, H—OH like bond distance of ~2.036–2.331 Å and O—H—C bond angle of ~180°; transition states present an H—C like bond distance of approximately ~1.386–1.403 Å, H—OH like bond distance of ~1.386 to 1.423 Å and O—H—C bond angle of ~180° (see Figs. 2, 3, 5 and 8).

3.3. Reaction with NO_3

All the energies values for the reaction of DMF/DMA with NO3 are summarized in Table 2c, Table 3 and Table 4c, Table 5 for DMF and DMA, respectively. The same mechanism as for OH radical and Cl atom, NO_3 radical involves hydrogen transfer from DMF (H_{1-6}/H_7), via the H-bonded complexes $(DMF\text{-}NO3)_{1-2}/(DMF\text{-}NO3)_3$ (gain in energy ~1.2–2.6 kcal mol^{-1}) and $TS_{1-6}NO3$ (abstraction of H_{1-6}) and $TS_{7-9}NO3$ (abstraction of H_{7-9}) to form $DMFR_{1-2}$, $DMFR_3$ and H_2O. The energies of $TS_{1-6}NO3$ and TS_7NO3 are ~23.4–29.5 kcal mol^{-1} higher than the total energy of the reactants.

Hydrogen transfer from DMA (H_{1-6}/H_{7-9}), also undergo via the H-bonded complexes $(DMA\text{-}NO3)_{1-2}/(DMA\text{-}NO3)_2$ (gain in energy ~1.1–4.4) and $TS_{1-6}NO3$ (abstraction of

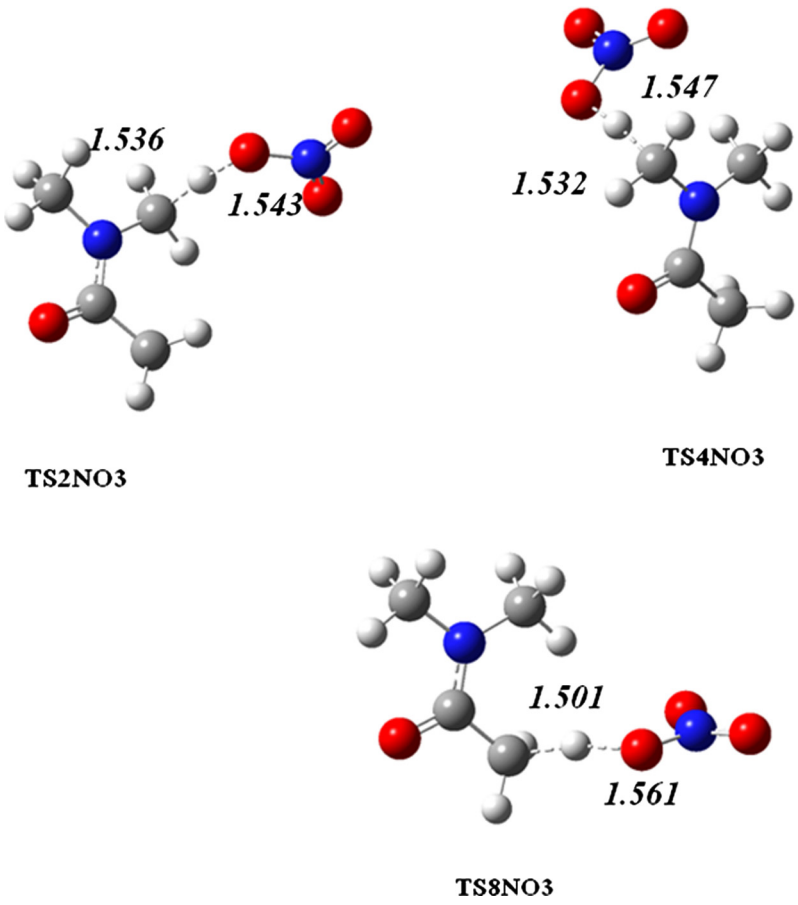

Figure 9 Structures of key species (TS) for reaction DMA + NO_3 considered for kinetics simulations determined by B3LYP/6-311++G(2d,pd), bond lengths in Angstrom.

Table 1 Energies of reactants and product species involved in the mechanism: In hartrees (E) as obtained from the DFT calculation. CBS-H enthalpy at 2 98.15 K. CBS-G Gibbs free energy at 298.15 K. CBS-E energy.CBS (0 K) energy at 0 K. (1) CRC Handbook of Chemistry and Physics New York October 2003.

Structure	CBS-H	CBS-G	CBS-E	CBS (0 K)	[a]$\Delta_f H^\circ_{0\ K}$	[b]$D_0{}^\circ$	[c]$\Delta_f H^\circ_{298\ K}$	[d]$\Delta_f H_{298K\ exp}$
DMF	−248,086694	−248,126146	−248,087638	−248,094697	−102,84	1145,71	−107,72	−57,18
DMFR1	−247,439139	−247,480126	−247,440083	−247,447444	−61,95	1053,19	−65,63	/
DMFR2	−247,439867	−247,476245	−247,440811	−247,446856	−61,59	1052,83	−66,09	/
DMFR3	−247,437721	−247,477928	−247,438665	−247,445759	−60,90	1052,14	−64,74	/
DMA	−287,316366	−287,361702	−287,31731	−287,326113	−109,64	1425,75	−115,69	−54,45
DMAR1	−286,67258	−286,713904	−286,673524	−286,681402	−70,34	1334,82	−75,97	/
DMAR2	−286,668882	−286,712959	−286,669826	−286,678467	−68,50	1332,98	−73,65	/
DMAR2	−286,660345	−286,704417	−286,661289	−286,670029	−63,21	1327,69	−68,29	/
OH	−75,646391	−75,666626	−75,647335	−75,650025	8,83	101,79	9,06	8,11
H2O	−76,333682	−76,355108	−76,334627	−76,337462	−57,28	219,53	−57,96	−65.24
Cl	−459,681244	−459,699282	−459,682189	−459,684945	28,59	0,00	29,81	28,97
HCl	−460,344858	−460,366043	−460,345802	−460,348162	−22,31	102,53	−22,35	−22,04
NO3	−279,915987	−279,947547	−279,916931	−279,920867	−43,88	333,38	−44,98	−45,60
HNO3	−280,575158	−280,605441	−280,576102	−280,579674	−92,02	433,15	−94,35	−31,98

[a] Heat of formation at 0 K in kcal mol^{-1}.
[b] Atomization energy in kcal mol^{-1} at 0 K.
[c] Heat of formation at 298.15 K in kcal mol^{-1}.
[d] Experimental Heat of formation at 298.15 K in kcal mol^{-1}.

Table 2 TS's and Complexes involved in the DMF + X reaction. CBS-H enthalpy at 298.15 K, CBS-G Gibbs free energy at 298.15 K, CBS-E: CBS energy at 0 K. TSn_X: Transition State, n: represents the position of H to abstract. X represents Cl, OH and NO_3.

Structure	CBS-H	CBS-G	CBS-E	CBS (0 K)	[a]$\Delta_f H^\circ_{0\ K}$	[b] $D_0°$	[c]$\Delta_f H^\circ_{298\ K}$	Freq (cm^{-1})
$(DMF\text{-}Cl)_1$	−707,78325	−707,818029	−707,775194	−707,783299	−76,55	1148,01	−87,52	/
$(DMF\text{-}Cl)_2$	−707,78325	−707,818029	−707,775194	−707,783299	−76,55	1148,01	−87,52	/
$(DMF\text{-}Cl)_3$	−707,78555	−707,816216	−707,772999	−707,781379	−75,34	1146,80	−88,96	/
$TS_{1–3}Cl$	−707,756155	−707,828121	−707,785609	−707,755422	−59,05	1130,51	−70,51	−696.651
$TS_{4–6}Cl$	−707,75551	−707,831068	−707,786971	−707,76405	−64,47	1135,93	−70,11	−1205.32
$TS7_{CL}$	−707,759998	−707,831521	−707,790143	−707,76781	−66,83	1138,29	−72,92	−402.74
$(DMF\text{-}OH)_1$	−323,749803	−323,764688	−323,723747	−323,731745	−85,87	1239,36	−109,15	/
$(DMF\text{-}OH)_2$	−323,749803	−323,764688	−323,723747	−323,731745	−85,87	1239,36	−109,15	/
$(DMF\text{-}OH)_3$	−323,744194	−323,759956	−323,720138	−323,727560	−83,25	1236,74	−105,63	/
$TS_{1–3}OH$	−323,726025	−323,768896	−323,726969	−323,735314	−88,11	1241,60	−94,23	−2002,67
$TS_{4–6}OH$	−323,724339	−323,767216	−323,725283	−323,733632	−87,06	1240,55	−93,17	−2040,97
TS_7OH	−323,708629	−323,772396	−323,729573	−323,735376	−88,15	1241,64	−83,32	−1931,28
$(DMF\text{-}NO3)_1$	−528,004628	−528,034152	−527,985570	−527,985570	−127,90	1460,27	−153,92	/
$(DMF\text{-}NO3)_2$	−528,004628	−528,034152	−527,985570	−527,985570	−127,90	1460,27	−153,92	/
$(DMF\text{-}NO3)_3$	−528,006890	−528,044850	−527,990830	−528,002400	−138,46	1470,83	−155,34	/
$TS_{1–3}NO3$	−527,955642	−528,046967	−527,996317	−528,006890	−141,28	1473,65	−123,18	−457,13
$TS_{4–6}NO3$	−527,956078	−528,048754	−527,997022	−528,007507	−141,67	1474,04	−123,45	−795,39
$TS7_{NO3}$	−527,965372	−528,048375	−527,997654	−528,007203	−141,48	1473,85	−129,29	−248,58

[a] Heat of formation at 0 K in kcal mol^{-1}.
[b] Atomization energy in kcal mol^{-1} at 0 K.
[c] Heat of formation at 298.15 K in kcal mol^{-1}.

Table 3 TS's and Complexes involved in the DMA + X reaction. CBS-H enthalpy at 298.15 K, CBS-G Gibbs free energy at 298.15 K, CBS-E: CBS energy at 0 K. TSn_X: Transition State, n: represents the position of H to abstract. X represents Cl, OH and NO_3.

Structure	CBS-H	CBS-G	CBS-E	CBS (0 K)	[a]$\Delta_f H^\circ_{0\ K}$	[b]$D_0°$	[c]$\Delta_f H^\circ_{298\ K}$	Freq (cm^{-1})
$(DMA\text{-}CL)_1$	−747,005271	−747,010981	−746,966216	−746,974805	−58,30	1403,00	−90,65	/
$(DMA\text{-}CL)_2$	−747,005271	−747,010981	−746,966216	−746,974805	−58,30	1403,00	−90,65	/
$(DMA\text{-}CL)_3$	−747,009108	−747,022848	−746,978053	−746,986921	−65,90	1410,60	−93,06	/
$TS_{1–3}Cl$	−746,980879	−747,067380	−747,019136	−747,009022	−79,77	1424,47	−75,35	−566,83
$TS_{4–6}Cl$	−746,990342	−747,067465	−747,019031	−747,006730	−78,33	1423,03	−81,29	−753,13
$TS_{7–9}Cl$	−746,991150	−747,050087	−747,004957	−746,983090	−63,50	1408,20	−81,79	−757,1
$(DMA\text{-}OH)_1$	−362,974876	−362,988692	−362,94582	−362,954604	−87,30	1514,03	−114,24	/
$(DMA\text{-}OH)_2$	−362,974876	−362,988692	−362,94582	−362,954604	−87,30	1514,03	−114,24	/
$(DMA\text{-}OH)_3$	−362,973393	−363,009435	−362,964337	−362,954446	−87,20	1513,93	−113,31	/
$TS_{1–3}OH$	−362,939698	−362,99617	−362,950642	−362,960498	−91,00	1517,73	−92,16	−2082,04
$TS_{4–6}OH$	−362,938803	−362,996399	−362,949747	−362,959901	−90,62	1517,35	−91,60	−1771,27
$TS_{7–9}OH$	−362,938066	−362,011543	−362,96011	−362,951579	−85,40	1512,13	−91,14	−2280,63
$(DMA\text{-}NO3)_1$	−567,234061	−567,278781	−567,220550	−567,233515	−145,07	1750,68	−161,40	/
$(DMA\text{-}NO3)_2$	−567,234061	−567,278781	−567,220550	−567,233515	−145,07	1750,68	−161,40	/
$(DMA\text{-}NO3)_3$	−567,239265	−567,266216	−567,215209	−567,237150	−147,35	1752,96	−163,68	/
$TS_{1–3}NO3$	−567,185273	−567,269313	−567,220604	−567,183160	−113,47	1719,08	−129,80	−1684,4
$TS_{4–6}NO3$	−567,185673	−567,266236	−567,217645	−567,183030	−113,39	1719,00	−129,72	−1526,47
$TS_{7–9}NO3$	−567,194973	−567,222725	−567,172622	−567,186584	−115,62	1721,23	−131,96	−1409,5

[a] Heat of formation at 0 K in kcal mol^{-1}.
[b] Atomization energy in kcal mol^{-1} at 0 K.
[c] Heat of formation at 298.15 K in kcal mol^{-1}.

H6) and $TS_{7–9}NO3$ (abstraction of H9) (barrier high ~23.4–29.5 kcal mol^{-1}) to form $DMAR_{1–2}$, $DMAR_3$ and H_2O.

For NO_3 radical, complexes are characterized by an H—C bond distance of approximately ~1.02–1.141 Å, (NO_2)O—H like bond distance of ~1.875–2.031 Å and O—H—C bond angle of ~180°; transition states present an H—C like bond distance of approximately ~1.386–1.423 Å, (NO_2)O—H like bond distance of ~1.386–1.423 Å and O—H—C bond angle of ~180° (see Figs. 2, 3, 6 and 9).

Table 4 ΔCBS-H enthalpy at 298.15 K (in kcal/mol) of reaction DMF + X radicals (OH, Cl and NO_3).

Structure	Cl	OH	NO_3
	ΔCBS-H		
DMF + X	0,00	0,00	0,00
(DMF−X)1	−9,61	−10,49	−1,22
(DMF−X)2	−9,61	−10,49	−1,22
(DMF−X)3	−11,05	−6,97	−2,64
TS1−3X	7.39	4.43	29.52
TS4−6X	7.80	5.49	29.24
TS7X	4.98	15.35	23.41
DMFR1 + HX	−10,08	−24,93	−18,28
DMFR2 + HX	−10,53	−25,39	−18,28
DMFR3 + HX	−9,19	−24,04	−13,88

Table 5 ΔCBS-H enthalpy at 298.15 K (in kcal/mol) of reaction of DMA + X radicals (OH, NO_3 and Cl atom).

Structure	Cl	OH	NO_3
	ΔCBS-H		
DMA + X	0,00	0,00	0,00
(DMA−X)1	−4,81	−7,60	−1,12
(DMA−X)2	−4,81	−7,60	−1,12
(DMA−X)3	−7,22	−6,67	−4,39
TS1−3X	10.50	14.47	29.49
TS4−6X	4.56	15.03	29.24
TS7−9X	4.05	15.49	23.41
DMAR1 + HX	−10,08	−24,94	−7,35
DMAR2 + HX	−10,08	−24,94	−7,35
DMAR3 + HX	−5,32	−20,18	−2,58

4. Kinetics

The mechanism of H-abstraction reaction of amide with X (OH, Cl, NO_3) radicals is examined as a competition between, two H-abstractions as follows:

$$Amide + X \underset{k_{-Ia}}{\overset{\vec{k}_{Ia}}{\leftarrow}} (Amide - X)_I \xrightarrow{\vec{k}_{Ib}} P1 + HX \quad Channel(I)$$

$$\underset{k_{-IIa}}{\overset{\vec{k}_{IIa}}{\leftarrow}} (Amide - X)_{II} \xrightarrow{\vec{k}_{IIb}} P2 + HX \quad Channel(II)$$

According to the reaction profiles, the rate constant (k) resultant to all the studied reaction channels can be analyzed in terms of conventional TST or RKM/master equation calculations. k_{Ia}, k_{IIa} are the forward rates and k_{-Ia}, k_{-IIa} reverse ones for the first step and k_{Ib}, k_{IIb} corresponds to the second steps respectively for channel *I* and channel *II*. On the basis of this hypothesis, rate constants of the channel *I* and *II* (k_I and k_{II}) can be expressed as follows:

$$k_I = \frac{k_{Ia} \times k_{Ib}}{k_{-Ia} + k_{Ib}} \quad with\ k_I = k_{eqI} \times k_{Ib} \quad (a)$$

$$k_{II} = \frac{k_{IIa} \times k_{IIb}}{k_{-IIa} + k_{IIb}} \quad with\ k_{II} = k_{eqII} \times k_{IIb} \quad (b)$$

where k_{eqI} and k_{eqII} (equation (a) and (b)) are the equilibrium constants between the isolated reactants and the complexes for channel *I* and channel *II* respectively.

All rate constants (k_{Ia}, k_{-Ia}, k_{Ib}, k_{IIa}, k_{-IIa} *and* k_{IIb}) involved in the H-abstraction reaction mechanism were calculated with ChemRate program (Mokrushin et al., 2002). Simulations were performed at pressure 1 atm and temperatures range 273–380 K. Collisional energy transfer was described using an exponential- down model, with ΔE_{down} = 300 cm^{-1}, Ar as a bath gas with lennard-jones parameters of σ = 4.4 and ξ = 216 K (Miyoshi, 2010; Galano, 2006). All rate constants quoted in this study are in s^{-1} or cm^3 $molecule^{-1}$ s^{-1} units.

In this case, the overall rate constant (c), the branching ratios (d) obtained from theoretical kinetic simulation are calculated as follows:

$$k_{overall} = k_I + k_{II} \quad (c)$$

$$\beta_I = \frac{k_I}{k_I + k_I} \quad and \quad \beta_{II} = 1 - \beta_I \quad (d)$$

Table 6a Rate constants (cm^3 $molecule^{-1}$ s^{-1}) and branching ratio (β_{II}) within the temperature range 273–380 for reaction DMF + Cl.

T	k_I ($\times 10^{-10}$)	k_{II} ($\times 10^{-10}$)	$k_{overall}$ ($\times 10^{-10}$)	[a] ($\times 10^{-10}$)	β_{II}
273	6,43785	6,81863	13,25648		0,51
280	6,51945	6,85438	13,37383		0,51
290	6,63435	6,90625	13,5406		0,51
298	**6,7248**	**6,9485**	**13,6733**	**1,9**	**0,51**
300	6,7473	6,95916	13,70646		0,51
310	6,8583	7,01272	13,87102		0,51
313	6,8913	7,02884	13,92014		0,50
320	6,96765	7,0668	14,03445		0,50
330	7,0752	7,1214	14,1966		0,50
333	7,10715	7,13791	14,24506		0,50
340	7,18125	7,17639	14,35764		0,50
350	7,28565	7,23164	14,51729		0,50
353	7,3167	7,24828	14,56498		0,50
360	7,38855	7,28715	14,6757		0,50
380	7,5903	7,39856	14,98886		0,49

[a] Rate constants of Solignac et al. (2005).

4.1. Kinetics results

4.1.1. DMF + X reaction

The H-abstraction reaction from DMF has been modeled as described above according to a complex mechanism in the entrance channel: two complexes $(DMF\text{-}X)_{1-2}$ and $(DMF\text{-}X)_3$ have been considered with the lowest two transition states for each atom/radical X involved .

For the Cl atom, the H-abstraction from the $((CH_3)_2N—)$ group site leads to the species $DMFR_{1-2}$ passing through $TS_{1-6}Cl$. The H- abstraction from the (—C(O)H) group leads to $DMFR_3$ through the transition state TS_7Cl. This path was found to be slightly more dominant with a branching ratio $\beta_{II} = 0.51$. Almost no temperature effect was observed for k_I *and* k_{II}. Calculated values of $k_{overall}$ vary from *1.32 (E−9) to 1.49 (E−09)* $cm^3\ molecule^{-1}\ s^{-1}$ in the temperature range 273–380 K (see Table 6a). The linear least square fit of all the data points provided by the calculation at different temperatures leads to the following Arrhenius expression:

$$k_{overall}(T) = 2.03 * 10^{-09} * exp\left(-\frac{118.18}{T}\right) cm^3\ molecule^{-1}\ s^{-1}$$

The dominant mechanistic channel of the reaction of DMF with OH-radicals involves the abstraction of a H-atom from the $((CH_3)_2N—)$ group and proceeds through the $TS_{1-6}OH$ transition state with β_I values varying between 0.95 and 0.90 in the temperature range 273–380 K. The H-abstraction from the (—C(O)H) group involves the TS_7OH transition state and leads to a k_I value ~20 times greater than that of k_{II} (see Table 6b). A small negative temperature dependence was observed for k_I and k_{II}. The $k_{overall}$ values range from *8.44 (E−11) to 7.59 (E−11)* $cm^3\ molecule^{-1}\ s^{-1}$ in the temperature domain cited above. The Arrhenius expression obtained from these values is as follows:

$$k_{overall}(T) = 5.78 * 10^{-11} * exp\left(\frac{103.54}{T}\right) cm^3\ molecule^{-1}\ s^{-1}$$

The results obtained concerning the reaction of NO_3 radicals with DMF show that the dominant mechanistic channel involves the abstraction of a H-atom from the (—C(O)H) group. This mechanism proceeds via the TS_7NO3 transition state and the corresponding β_{II} values vary between 0.91 and 0.85 in the temperature range 273–380 K. Contrary to the result obtained for OH, the H-abstraction from the $((CH_3)_2N)—)$ group involving $TS_{1-6}NO3$ leads to a k_{II} value ~10 times greater than that of k_I (see Table 6c). A negative temperature dependence of rate constants k_I and k_{II} was observed. The $k_{overall}$ values range from *2.09 (E−13) to 7.82 (E−15)* $cm^3\ molecule^{-1}\ s^{-1}$ in the temperature range used in the calculation. The following Arrhenius expression of $k_{overall}$ between 273 and 380 K is obtained using least-squares fit:

$$k_{overall}(T) = 1.82 * 10^{-18} * exp\left(\frac{3184.1}{T}\right) cm^3 molecule^{-1}\ s^{-1}$$

4.1.2. DMA + X reaction

As in the case DMF, two complexes $(DMA\text{-}X)_{1-2}$ and $(DMA\text{-}X)_3$ have been considered with the lowest two transition states for each atom/radical X involved.

For the DMA + Cl system, the H-abstraction from the $((CH_3)_2N—)$ group leads to the species $DMAR_{1-2}$ via $TS_{1-6}Cl$. The H-abstraction from the $(—C(O)CH_3)$ group leads to $DMAR_3$ species through $TS_{7-9}Cl$. The channel (II) was found to be the dominant path with branching ratio values ranging from 0.71 to 0.64 and the k_{II} value ~2 times greater than that of k_I. Almost no temperature effect was observed on the rate constants. The calculated values of $k_{overall}$ vary from *1.20 (E−9) to 1.35 (E−9)* $cm^3\ molecule^{-1}\ s^{-1}$ in the temperature range 273–380 K (see Table 7a). The Arrhenius expression obtained from these values is as follows:

$$k_{overall}(T) = 1.82 * 10^{-09} * exp\left(-\frac{116.65}{T}\right) cm^3\ molecule^{-1}\ s^{-1}$$

The same tendency observed for the reaction of OH with DMF is also observed for DMA. The channel (*I*) was found to be largely dominant with a branching ratio β_I value equal to ≈ 0.98 and k_I almost ~40 times greater than k_{II}. In addition, a small negative temperature effect on the $k_{overall}$ rate constant values was obtained. In the temperature range 273–380 K (see Table 7b), the Arrhenius expression obtained for $k_{overall}$ is as follows:

$$k_{overall}(T) = 5.04 * 10^{-11} * exp\left(\frac{153.23}{T}\right) cm^3\ molecule^{-1}\ s^{-1}$$

For the reaction of NO_3 with DMA, reaction path (II) was found to be slightly more dominant with a branching ratio β_{II} varying slightly between 0.62 and 0.59. In this case k_{II} is equal to ~1.4 times k_I. (see Table 7c). An important negative temperature coefficient is obtained for $k_{overall}$ in the temperature range 273–380 K. Therefore, the Arrhenius expression obtained for $k_{overall}$ is as follows:

$$k_{overall}(T) = 2.82 * 10^{-18} * exp\left(\frac{1564.2}{T}\right) cm^3\ molecule^{-1}\ s^{-1}$$

5. Discussion

5.1. Structure and reactivity

For OH reaction, the major channel appears to be the abstraction from methyl groups related to the nitrogen atom in DMF/DMA, channel **I** with the branching ratio β_I ~0.96 and ~0.98 respectively. Moreover, same reactivity is observed for both molecules (DMF and DMA) with OH where $k_{overall}$ (DMA) ~$k_{overall}$ (DMF).

In opposite way reaction with Cl present the same reactivity for both molecules with the channel **II** slightly the dominant path. In addition supplement in reactivity toward electrophilic attack with rising methyl substitution due to the positive inductive effect of these groups can be stated for this reaction. In fact the branching ratio $\boldsymbol{\beta_{II}}$ passes from ~0.50 for DMF to ~0.70 for DMA.

Concerning the reaction with nitrate radicals, from the branching ratio values, it is clear to note that channel **II** is the dominant path; this can be explained by sterical effect of the NO_3 structure for reaction with DMF, and this hypothesis is confirmed in the reaction of DMA with NO_3. In fact, the branching ratio β_{II} passes from ~0.90 to ~0.60, when H in (C(O)H) group is replaced by CH_3, which makes the

Table 6b Rate constants (cm^3 $molecule^{-1}$ s^{-1}) and branching ratio (β_I) within the temperature range 273–380 for reaction DMF + OH.

T	k_I ($\times 10^{-11}$)	k_{II} ($\times 10^{-12}$)	$k_{overall}$ ($\times 10^{-11}$)	[a]($\times 10^{-11}$)	β_I
273	8,02295	4,21692	8,444642		0,95
280	7,92246	4,46412	8,368872		0,95
290	7,78531	4,81728	8,267038		0,94
298	**7,68053**	**5,0988**	**8,19041**	**1,4**	**0,94**
300	7,65505	5,16888	8,171938		0,94
310	7,53103	5,5182	8,08285		0,93
313	7,49502	5,62236	8,057256		0,93
320	7,41299	5,86404	7,999394		0,93
330	7,30015	6,20568	7,920718		0,92
333	7,26739	6,30732	7,898122		0,92
340	7,1916	6,54252	7,845852		0,92
350	7,08929	6,87396	7,776686		0,91
353	7,05926	6,97224	7,756484		0,91
360	6,9901	7,19952	7,710052		0,91
380	6,80472	7,83156	7,587876		0,90

[a] Rate constants of Solignac et al. (2005).

Table 6c Rate constants (cm^3 $molecule^{-1}$ s^{-1}) and branching ratio (β_{II}) within the temperature range 273–380 K of Reaction DMF + NO_3 Radical.

T	k_I ($\times 10^{-14}$)	k_{II} ($\times 10^{-14}$)	$k_{overall}$ ($\times 10^{-14}$)	[a]($\times 10^{-14}$)	β_{II}
273	**1,83952**	**19,0998**	**20,93932**	**3,4**	**0,91**
280	1,45432	14,283	15,73732		0,91
290	1,05808	9,6498	10,70788		0,90
298	**0,83168**	**7,17273**	**8,00441**	**4,5**	**0,90**
300	0,784488	6,67494	7,459428		0,89
310	0,591704	4,71807	5,309774		0,89
313	**0,545392**	**4,26834**	**4,813732**	**5,6**	**0,89**
320	0,453312	3,4011	3,854412		0,88
330	0,35228	2,49615	2,84843		0,88
333	**0,327456**	**2,2824**	**2,609856**	**7,5**	**0,87**
340	0,27736	1,86228	2,13964		0,87
350	0,221	1,41048	1,63148		0,86
353	**0,206896**	**1,30122**	**1,508116**	**13,9**	**0,86**
360	0,178	1,08324	1,26124		0,86
380	0,11904	0,66312	0,78216		0,85

[a] Rate coefficient of El Dib and Chakir (2007).

Table 7a Rate constants (cm^3 $molecule^{-1}$ s^{-1}) and branching ratio (β_{II}) within the temperature range 273–380 K of Reaction DMA + CL.

T	k_I ($\times 10^{-10}$)	k_{II} ($\times 10^{-10}$)	$k_{overall}$ ($\times 10^{-10}$)	[a]($\times 10^{-10}$)	β_{II}
273	3,4398	8,55699	11,99679		0,71
280	3,53835	8,55283	12,09118		0,71
290	3,6774	8,55192	12,22932		0,70
298	**3,78705**	**8,55478**	**12,34183**	**2,5**	**0,69**
300	3,81435	8,55595	12,3703		0,69
310	3,94905	8,56427	12,51332		0,68
313	3,9891	8,56752	12,55662		0,68
320	4,0818	8,57636	12,65816		0,68
330	4,21245	8,59183	12,80428		0,67
333	4,2513	8,59716	12,84846		0,67
340	4,3413	8,61029	12,95159		0,66
350	4,4682	8,63135	13,09955		0,66
353	4,506	8,63811	13,14411		0,66
360	4,5933	8,65475	13,24805		0,65
380	4,83825	8,7074	13,54565		0,64

[a] Rate coefficient of Solignac et al. (2005).

Table 7b Rate constants (cm^3 $molecule^{-1}$ s^{-1}), branching ratio (β_I) within the temperature range 273–380 K of Reaction DMA + OH.

T	k_I ($\times 10^{-11}$)	k_{II} ($\times 10^{-12}$)	$k_{overall}$ ($\times 10^{-11}$)	[a]($\times 10^{-11}$)	β_I
273	8,58767	2,14908	8,802578		0,98
280	8,4864	2,10648	8,697048		0,98
290	8,34782	2,0484	8,55266		0,98
298	**8,24161**	**2,00412**	**8,442022**	**1,9**	**0,98**
300	8,21574	1,99344	8,415084		0,98
310	8,08977	1,94112	8,283882		0,98
313	8,05311	1,926	8,24571		0,98
320	7,96939	1,89156	8,158546		0,98
330	7,85421	1,84428	8,038638		0,98
333	7,82054	1,8306	8,0036		0,98
340	7,74384	1,79928	7,923768		0,98
350	7,63802	1,75644	7,813664		0,98
353	7,60708	1,74396	7,781476		0,98
360	7,53649	1,71552	7,708042		0,98
380	7,34487	1,63908	7,508778		0,98

[a] Rate coefficient of Solignac et al. (2005).

Table 7c Rate constants (cm^3 $molecule^{-1}$ s^{-1}) and branching ratio (β_{II}) within the temperature range 273–380 K of Reaction DMA + NO_3.

T	k_I ($\times 10^{-14}$)	k_{II} ($\times 10^{-14}$)	$k_{overall}$ ($\times 10^{-14}$)	[a]($\times 10^{-14}$)	β_{II}
273	**3,24224**	**5,32395**	**8,56619**	**2,3**	**0,62**
280	2,84576	4,61934	7,4651		0,62
290	2,38416	3,8106	6,19476		0,62
298	**2,08456**	**3,29319**	**5,37775**	**4,9**	**0,61**
300	2,01768	3,17853	5,19621		0,61
310	1,7232	2,67822	4,40142		0,61
313	**1,64632**	**2,54871**	**4,19503**	**5,2**	0,61
320	1,48408	2,27745	3,76153		0,61
330	1,28792	1,953	3,24092		0,60
333	**1,236**	**1,86786**	**3,10386**	**8,24**	**0,60**
340	1,12552	1,68777	2,81329		0,60
350	0,99	1,46889	2,45889		0,60
353	**0,95368**	**1,41075**	**2,36443**	**13,9**	**0,60**
360	0,87592	1,28673	2,16265		0,59
380	0,696864	1,00503	1,701894		0,59

[a] Rate coefficient of El Dib and Chakir (2007).

approaches in the H-abstraction more difficult in the case of (C(O)CH_3) group.

5.2. Comparison with experimental data

Only one experimental study, at room temperature (Solignac et al., 2005) is found in the literature, concerning the reaction of DMF with Cl atoms and DMA with Cl atoms. The rate constants obtained in this study for the reaction of Cl with DMF/DMA are ~4–5 times greater than the values obtained experimentally respectively for DMF and DMA. Given that the energies calculations were determined with 2–3 kcal of uncertainties, values obtained in this work can be considered as in satisfactory agreement with the values of Solignac et al. (2005). Because of uncertainties associated with several parameters in these calculations and in the related experimental method, the goal of these calculations is therefore to determine whether or not the experimentally observed yields can be produced within the uncertainties of the calculations.

Concerning the reaction with NO_3 radicals, El Dib and Chakir (2007), have reported rate constants of 4.4×10^{-14} and 1.6×10^{-14} cm^3 $molecule^{-1}$ s^{-1} for the reactions of NO_3 with DMF and DMA, respectively at room temperature. The rate coefficients obtained in this study for the reaction of NO_3 with (DMA, DMF) are in satisfactory agreement with the experimental results obtained by El Dib and Chakir (2007). However, results from these calculations predict that the rate constant of the reaction of nitrate radicals with amides (DMF, DMA) decreases with temperature over the range 273–380 K, which is in good agreement with the experimental data.

The discrepancies between experimental observations and calculations may be a consequence of the uncertainties of both experimental determinations and theoretical calculations.

Two experimental determinations were found in the literature concerning the reaction between DMA and OH radicals (Koch et al., 1997; Solignac et al., 2005) and one experimental determination was found in the literature concerning the reaction between DMF and OH radicals (Solignac et al., 2005). As for the reactions of amides with chlorine atoms, our values are approximately 4 times greater than the values obtained experimentally. In addition, in their study to investigate the sites of attack of OH radicals on amides in an aqueous solution, Hayon et al. (1970) have found that for formamide, abstraction may occur from either the (CH_3—C(O)—) or the (NH_2—) moieties. Meanwhile, for other amides such as N-methylformamide and N,N-dimethylformamide, the abstraction was found to occur mostly from the N-methyl groups (Koch et al., 1997; Solignac et al., 2005; Rudic et al., 2003). This mechanistic tendency is also observed in our theoretical calculations.

6. Conclusion

This study represents the first theoretical determination of the rate coefficients and detailed mechanism for the reactions of OH, NO_3 radicals and Chlorine atoms with DMF/DMA, over a temperature range 273–380 K. This work has been carried out using DFT and CBS-QB3 methods, and this methods exposed to be the most efficient and accurate computational methods for the study of this type of reactions. Quantum calculations show that, the reactions of DMF/DMA with Cl, OH and NO_3 radicals are exothermic and the mechanism passes firstly through an intermediate complex more energetically stable than the reactants and secondly, the intermediate complex dissociates to form reaction product after passing through a transition state (TS).

Kinetic and mechanistic results indicate that the mechanism of the Cl reaction with amides goes mainly through H-atom transfer from the (C(O)H) and ($C(O)CH_3$) sites but the abstraction from the ($N(CH_3)_2$) is not negligible. The same conclusion can be drawn concerning the reaction of NO_3 with amides (DMF, DMA). In addition branching ratio is sensitive to the sterical effect of the NO_3 structure. Concerning the reaction of amides with OH radical calculation results show that the mechanism is mainly dominated by the hydrogen abstraction from the N-methyl groups. This mechanistic tendency is in agreement with the experimental results. The calculated overall rate constants are in reasonable agreement with the experimental ones, available in the literature.

References

Aschmann, M.S., Atkinson, R., 1999. Atmos. Environ. 33, 591–599.
Carter, W.P.L., 1994. J. Air Waste Manage. Assoc. 44, 881.
Coote, M.L., Wood, G.P.F., Radom, L., 2002. J. Phys. Chem. A 106, 12124.
Cremer, D., Kraka, E., Szalay, P.G., 1998. Chem. Phys. Lett. 292, 97.
Curtiss, L.A., Raghavachari, K., Redfern, P.C., Pople, J.A., 1997. J. Chem. Phys. 106, 1063.
da Silva, Gabriel., 2009. J. Chem. Theor. Comput. 5, 12.
Dybala-Defratyka, A., Paneth, P., Pu, J., Truhlar, D.G., 2004. J. Phys. Chem. A 108, 2475.
El Dib, G., Chakir, A., 2007. Atmos. Environ. 41, 5887–5896.
Fenske, J.D., Kuwata, K.T., Houk, K.N., Paulson, S.E., 2000a. J. Phys. Chem. A 104, 7246.
Fenske, J.D., Hasson, A.S., Paulson, S.E., Kuwata, K.T., Ho, A., Houk, K.N., 2000b. J. Phys. Chem. A 104, 7821.
Finlayson-Pitts, B.J., Pitts Jr., J.N., 1999. Chemistry of the Upper and Lower Atmosphere. Academic Press, California.
Galano, Annia, 2006. J. Phys. Chem. A 110 (29).
Frisch, M.J., Trucks, G.W., Schlegel, H.B., Scuseria, G.E., Robb, M. A., Cheeseman, J.R., Scalmani, G., Barone, V., Mennucci, B., Petersson, G.A., Nakatsuji, H., Caricato, M., Li, X., Hratchian, H. P., Izmaylov, A.F., Bloino, J., Zheng, G., Sonnenberg, J.L., Hada, M., Ehara, M., Toyota, K., Fukuda, R., Hasegawa, J., Ishida, M., Nakajima, T., Honda, Y., Kitao, O., Nakai, H., Vreven,T., Montgomery, J.A., Jr., Peralta, J.E., Ogliaro, F., Bearpark, M., Heyd, J.J., Brothers, E., Kudin, K.N., Staroverov, V.N., Keith, T., Kobayashi, R., Normand, J., Raghavachari, K., Rendell, A., Burant, J.C., Iyengar, S.S., Tomasi, J., Cossi, M., Rega, N., Millam, J.M., Klene, M., Knox, J.E., Cross, J.B., Bakken, V., Adamo, C., Jaramillo, J., Gomperts, R., Stratmann, R.E., Yazyev, O., Austin, A.J., Cammi, R., Pomelli, C., Ochterski, J.W., Martin, R.L., Morokuma, K., Zakrzewski, V.G., Voth, G.A., Salvador, P., Dannenberg, J.J., Dapprich, S., Daniels, A.D., Farkas, O., Foresman, J.B., Ortiz, J.V., Cioslowski, J., Fox, D.J., 2010. Gaussian 09, Revision B.01, Gaussian, Inc., Wallingford CT.
Gonzalez, C., Schlegel, H.B., 1989. J. Chem. Phys. 90, 2154.
Gonzalez, C., Schlegel, H.B., 1990. J. Phys. Chem. 94, 5523.
Gutbrod, R., Schindler, R.N., Kraka, E., Cremer, D., 1996. Chem. Phys. Lett. 252, 221.
Hayon, E., Ibata, T.N., Lichtin, N., Simic, M., 1970. J. Am. Chem. Soc. 92, 3898–3903.
Knyazev, V.D., Tsang, W., 1999. J. Phys. Chem. A 103, 3944.
Knyazev, V.D., Tsang, W., 2000. J. Phys. Chem. A 104, 10747.
Koch, R., Palm, W.U., Zetzsch, C., 1997. Int. J. Chem. Kinet. 29, 81–87.
Kroll, J.H., Sahay, S.R., Anderson, J.G., Demerjian, K.L., Donahue, N.M., 2001. J. Phys. Chem. A 105, 4446.
Kuwata, K.T., Templeton, K.L., Hasson, A.S., 2003. J. Phys. Chem. A 107, 11525.
Lee, C., Yang, W., Parr, R.G., 1988. Phys. Rev. B 37, 785.
Malick, D.K., Petersson, G.A., Montgomery Jr., J.A., 1998. J. Chem. Phys. 108, 5704.
Manahan, S.E., 1994. Environmental Chemistry. Lewis, London.
Miyoshi, Akira, 2010. Int. J. Chem. Kinet. 42 (5), 273–288.
Mokrushin V, Bedanov V, Tsang W, Zachariah MR, Knyazev VD, 2002. CHEMRATE, Version 1.19, National Institute of Standards and Technology, Gaithersburg, MD.
Montgomery, J.A., Frisch, M.J., Ochterski, J.W., Peterson, G.A., 1999. J. Chem. Phys. 110, 2822.
Olzmann, M., Kraka, E., Cremer, D., Gutbrod, R., Andersson, S.J., 1997. Phys. Chem. A 101, 9421.
Robinson, P.J., Holbrook, K.A., 1972. Unimolecular Reactions. Wiley-Interscience, London.
Rudic, S., Murray, H.J.N.C., Orr-Ewing, A.J., 2003. Phys. Chem. Chem. Phys., 1205–1212
Solignac, G., Mellouki, A., Le Bras, G., Barnes, I., Benter, Th., 2005. J. Photochem. Photobiol., A 176, 136–142.
Stipa, P., 2001. J. Chem. Soc., Perkin Trans. 2, 1793.
Tiu, Gerald C., Tao, Fu-Ming, 2006. Chem. Phys. Lett. 428, 42–48.
Tokmakov, I.V., Lin, M.C., 2003. J. Am. Chem. Soc. 125, 11397.
Tokmakov, I.V., Lin, M.C., 2004. J. Phys. Chem. A 108, 9697.
Tsang, W., Bedanov, V., Zachariah, M.R., 1996. J. Phys. Chem. 100, 4011.
Tuazon, E.C., Atkinson, R., Aschmann, S.M., 1994. Res. Chem. Intermed. 20, 303.
Wood, G.P.F., Henry, D.J., Radom, L., 2003. J. Phys. Chem. A 107, 7985.
Zhang, D., Lei, W., Zhang, R., 2002. Chem. Phys. Lett. 358, 171.